

# Dynamic modeling and parameters identification of a spindle–holder taper joint

Chao Xu · Jianfu Zhang · Zhijun Wu ·  
Dingwen Yu · Pingfa Feng

Received: 7 May 2012 / Accepted: 24 October 2012 / Published online: 10 November 2012  
© Springer-Verlag London 2012

**Abstract** Dynamic behavior of spindle–holder taper joint is critical in the spindle system of machine tool, related to the machining process. The parameters of the holder joint are significant for the spindle–holder system. This paper developed a new approach to investigate the dynamic behavior of the taper joint in modeling and parameters identification. Firstly, dynamic model is illustrated in both radial and axial directions based on the pairs of spring and damping. And frequency response function is used to identify the unknown modal parameters of frequencies and damping ratios. Secondly, a platform is designed and manufactured to establish the testing system in order to investigate the taper joint. Furthermore, taper joint of a BT50 holder is investigated, and the pre-force at the end of holder is the main consideration during the testing. The results show that the dynamic stiffness increases with the increasing of pre-force at the end of the holder. In addition, the paper discusses the phenomenon in microstructure based on peak-hollows model and the joint parameters are proved to be workable through simulation. The joint parameters are instructive to the design and manufacturing of the spindle.

**Keywords** Taper joint · Dynamic modeling · Parameters identification · Machine tool

## 1 Introduction

The taper joint of spindle–holder is widely applied in spindle system of machine tool to support the holder and achieve automatic tool changing. David reported that about 25 to

50 % of the total deformation of the spindle system derived from spindle–holder taper joint [1]. Some researchers introduced that the chatter which would lead to poor surface quality especially in high-speed machining is related to the dynamic behavior of the spindle [2, 3]. The weak dynamic stiffness of the spindle–holder joint will influence the vibration of the spindle during the machining. The dynamic performance of spindle influences the machining process directly, which makes it necessary to study the behavior of spindle–holder joint [4, 5].

Literatures about spindle–holder system suggest that dynamic modeling and parameters identification are the major aspects to study the performance [6–8]. Several methods are used to investigate the issue, and the common way is to consider it as the assembly of linear springs and dampings [9, 10]. And the parameters are calculated from the frequency response function (FRF) which carries most information of the joint. It is necessary to predict the FRF of the spindle before a real machine tool is manufactured in order to shorten production cycle [11–15]. Moreover, the finite element method (FEM) is a popular way to simulate the dynamic system. But the boundary condition of contact cannot meet the requirements without an effective model, so it is significant to understand the joint condition of the spindle–holder joint. In addition, the receptance coupling (RC) is widely used to analyze the dynamics and predict FRF as well, which is applied in the tool point dynamics prediction, especially in high-speed machining [15, 16]; accordingly, the joint parameters of spring and damping are helpful to deduce the dynamic equations. Notably, Ertürk et al. [16–18] used averaged RC translational and rotational stiffness to describe the interface. Namazia [19] simplified the spindle and holder with Timoshenko beam element model, and the interface is regarded as uniformly distributed translational and rotational springs. In this way, it is difficult to apply in solid element FEM for the parameters focused on

C. Xu (✉) · J. Zhang · Z. Wu · D. Yu · P. Feng  
Department of Precision Instruments and Mechanology,  
Tsinghua University,  
Beijing, China 100084  
e-mail: xuchao.thu@gmail.com

the total effect. Hence, the joint parameters are the bottleneck to restrict the accuracy of simulation.

In this paper, a standard BT 50 spindle–holder joint is studied to explore the spindle–holder of dynamic model and parameters identification. This holder is widely used in actual using and its taper is standard 7/24 without self-locking [20]. And the pre-force at the end of the spindle–holder is the main consideration among all the influencing factors, which directly determines contact condition of joints.

## 2 Dynamic modeling

Dynamic model is to describe the characteristics of complex system, which is approximate to characteristics of the original one and contain unknown parameters. Then, it is necessary to obtain the unknown parameters from experiments and calculation. In addition, the model should be as simple as possible if the model can represent the true system to some extent. It is necessary to model the dynamic system, derivate the identification algorithm, obtain the predefined parameters, and simulate the dynamic characteristics during the whole analysis of the spindle–holder system.

Some assumptions are proposed to model the dynamic system. Firstly, the holder and spindle are Axially symmetric around the center. So it is enough to study one section separated by the plane through the central axis. Secondly, the deformations of holder and spindle themselves are assumed to be smaller than those of taper joint under forces. Therefore, the spindle and holder are regarded as rigid bodies. Additionally, the natural frequencies of unrestraint holder are higher than those with the taper joint considered.

From microscopic perspective, mechanical joint consists of innumerable interactional peak-hollow contacts due to the roughness surface generated from machining process or others [21], which is shown in Fig. 1. Each contact has the characteristic of elasticity and resistance when normal force was applied on the bodies. In other words, each small contact can be considered as a pair of spring and damping, and the total model can represent the original system if sufficient accuracy parameters of springs and damping are identified.

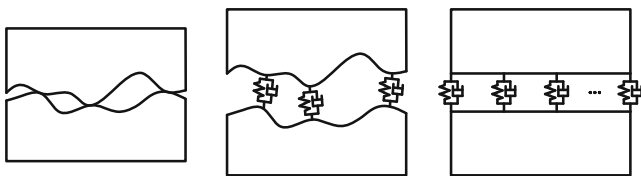


**Fig. 1** Microscopic description of mechanical joints

Moreover, peaks and hollows are distributed in the joint randomly and evenly. And the directions of spring and damping are perpendicular to the contact regions. The tangential effect of them is distributed randomly and evenly as well, which has less effect on the total normal direction. Therefore, the normal direction is the main constraint of the total effect. As a result, the pairs of normal spring and damping are equivalent to the micro regions and take the place of the whole joint.

In this paper, the dynamic characteristics of the BT50 (Fig. 2a) taper joint are the major consideration. The taper surface is the only contact region, shown in Fig. 2b. The pressure distributed in the taper joint is perpendicular to the normal surface, which is dragged by the pre-force at the end of the spindle–holder. Each contact region is regarded as both elastic and viscous element. In this way, the total effect of spindle–holder is equivalent to the innumerable degrees of freedom system with the direction perpendicular to the normal surface. However, it is difficult to analyze the complicated system without any simplifications. So it is necessary to simplify dynamic model to meet the requirements of calculation and simulation.

The spindle–holder system is analyzed in one axial direction and two radial directions in terms of structure feature and force conditions. In radial direction, the dynamic behaviors in  $X$  direction and  $Y$  direction are theoretically the same because the holder and spindle is Axially symmetric. There are two aspects to discuss: the location of spring and damping and the acquisition method of unknown parameters. The locations are determined by the vibration shapes under forces. In practice, the pressure or stress at the big end and small end are greater than that in the middle, which can be explained by the phenomena that the holder would be severely worn and torn after long time use. Moreover, the first several orders of modal shapes have something to do with the two support ends. In axial direction, the holder shows the only axial translation with a single

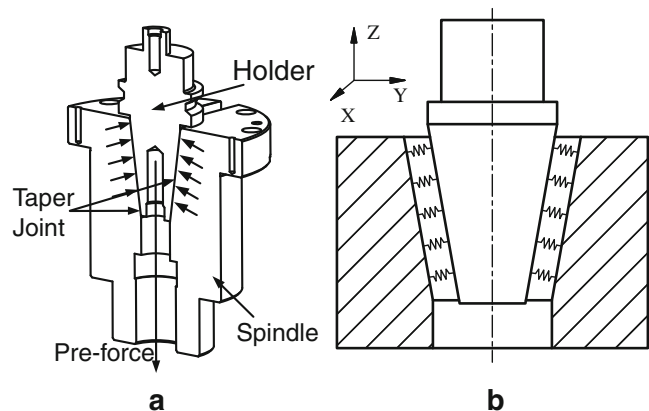


**Fig. 2** Analysis of spindle–holder joint

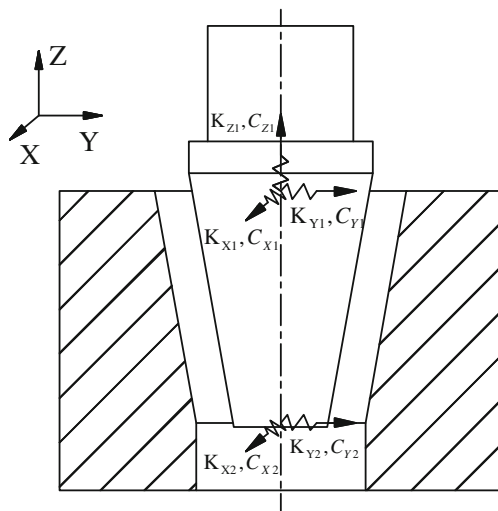


Fig. 3 Equivalent modeling of the spindle–holder system

degree of freedom. In this way, the dynamic model of taper joint is shown in Fig. 3.

Pairs of spring and damping are the virtual elements relevant to dynamic system, which is influenced by external conditions. The taper joint in radial direction is equivalent to the two pairs of spring and damping located at the big and small ends, respectively. And the axial restraint is connected by the spring and damping at the big end for the stability. As is well known, 6 degrees of freedom at least are needed to make an object fully constrained. The pairs of spring and damping constrain 5 degrees of freedom of the holder while another degree of freedom is fixed by the axial block.

### 3 Parameters identification method

The joint parameters identification method proposed in this paper is based on the experiment. The method is based on the FRFs between the locations of excitations and pickups, which can express the spindle–holder behaviors. Theoretically, the spindle–holder system is a whole system, so every point except the static modal nodes on the holder can express the dynamic characteristics which convey information influenced by the joint. Therefore, when excitation applies on the holder, most nodes on the holder will express all dynamic characteristics which couple with each other. So, it is available to study taper joint and obtain dynamic parameters by measuring the holder when the vibration signal is decoupled.

In radial direction, dynamic analysis for identification with stiffness and damping involved is proposed in Fig. 4. The mass and the moment of inertia of the holder are the  $m$  and  $I_x$ , respectively. After an excitation at a small tip in radial direction, the whole system will vibrate freely influenced by system including joint feature, where the modal characteristics are coupled and mixed in response.

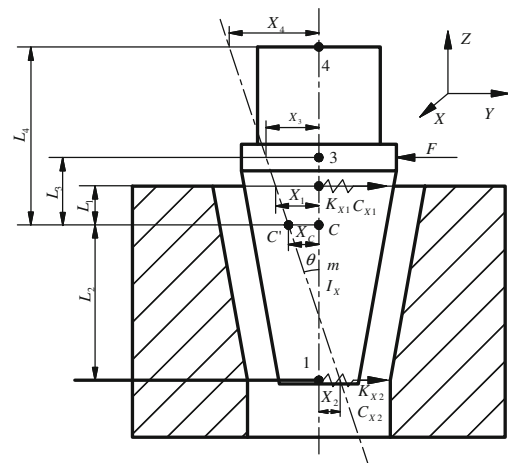


Fig. 4 Dynamic analysis in the radial direction

The holder in the model suggests two motions in this section: one is translation and the other is rotation.  $X_c$  and  $\theta$  are time-variant variables, which stand for displacement and angular displacement of the holder. The mass, damping and stiffness matrixes contain both the known geometric and property parameters and undetermined ones.

The dynamic equation of the radial section is presented as follows:

$$\begin{bmatrix} m \\ I_C \end{bmatrix} \begin{Bmatrix} \ddot{X}_c \\ \ddot{\theta} \end{Bmatrix} + \begin{bmatrix} C_{X1} + C_{X2} & C_{X1}L_1 + C_{X2}L_2 \\ C_{X1}L_1 - C_{X2}L_2 & C_{X1}L_1^2 - C_{X2}L_2^2 \end{bmatrix} \begin{Bmatrix} \dot{X}_c \\ \dot{\theta} \end{Bmatrix} + \begin{bmatrix} K_{X1} + K_{X2} & K_{X1}L_1 + K_{X2}L_2 \\ K_{X1}L_1 - K_{X2}L_2 & K_{X1}L_1^2 - K_{X2}L_2^2 \end{bmatrix} \begin{Bmatrix} X_c \\ \theta \end{Bmatrix} = 0 \tag{1}$$

Where, the mass matrix is

$$[M] = \begin{bmatrix} m \\ I_C \end{bmatrix} \tag{2}$$

The damping matrix is

$$\begin{aligned} [C] &= \begin{bmatrix} C_{X1} + C_{X2} & C_{X1}L_1 + C_{X2}L_2 \\ C_{X1}L_1 - C_{X2}L_2 & C_{X1}L_1^2 - C_{X2}L_2^2 \end{bmatrix} \\ &= \begin{bmatrix} C_{11} & C_{12} \\ C_{21} & C_{22} \end{bmatrix} \end{aligned} \tag{3}$$

The stiffness matrix is

$$\begin{aligned} [K] &= \begin{bmatrix} K_{X1} + K_{X2} & K_{X1}L_1 + K_{X2}L_2 \\ K_{X1}L_1 - K_{X2}L_2 & K_{X1}L_1^2 - K_{X2}L_2^2 \end{bmatrix} \\ &= \begin{bmatrix} K_{11} & K_{12} \\ K_{21} & K_{22} \end{bmatrix} \end{aligned} \tag{4}$$

Accordingly, the dynamic equations are simplified as follows:

$$\begin{bmatrix} m \\ I_C \end{bmatrix} \begin{Bmatrix} \ddot{X}_C \\ \ddot{\theta} \end{Bmatrix} + \begin{bmatrix} C_{11} & C_{12} \\ C_{21} & C_{22} \end{bmatrix} \begin{Bmatrix} \dot{X}_C \\ \dot{\theta} \end{Bmatrix} + \begin{bmatrix} K_{11} & K_{12} \\ K_{21} & K_{22} \end{bmatrix} \begin{Bmatrix} X_C \\ \theta \end{Bmatrix} = 0 \tag{5}$$

To change the form of the equations

$$\begin{cases} m \ddot{X}_C = -C_{11} \dot{X}_C - C_{12} \dot{\theta} - K_{11} X_C - K_{12} \theta \\ I_C \ddot{\theta} = -C_{21} \dot{X}_C - C_{22} \dot{\theta} - K_{21} X_C - K_{22} \theta \end{cases} \tag{6}$$

To make

$$u = [u_1, u_2, u_3, u_4]^T \tag{7}$$

where,  $u_1 = X_C, u_2 = \theta, u_3 = \dot{X}_C, u_4 = \dot{\theta}$

So, the second derivative of displacement and rotation angle is expressed as below:

$$\begin{cases} \ddot{X}_C = -\frac{C_{11}}{m} \dot{u}_3 - \frac{C_{12}}{m} \dot{u}_4 - \frac{K_{11}}{m} u_1 - \frac{K_{12}}{m} u_2 = \dot{u}_3 \\ \ddot{\theta} = -\frac{C_{21}}{I_C} \dot{u}_3 - \frac{C_{22}}{I_C} \dot{u}_4 - \frac{K_{21}}{I_C} u_1 - \frac{K_{22}}{I_C} u_2 = \dot{u}_4 \end{cases} \tag{8}$$

To make a new matrix with the above equations

$$\dot{u} = \begin{pmatrix} \dot{u}_1 \\ \dot{u}_2 \\ \dot{u}_3 \\ \dot{u}_4 \end{pmatrix} = \begin{bmatrix} 0 & 0 & 1 & 0 \\ 0 & 0 & 0 & 1 \\ -\frac{K_{11}}{m} & -\frac{K_{12}}{m} & -\frac{C_{11}}{m} & -\frac{C_{12}}{m} \\ -\frac{K_{21}}{I_C} & -\frac{K_{22}}{I_C} & -\frac{C_{21}}{I_C} & -\frac{C_{22}}{I_C} \end{bmatrix} \begin{pmatrix} u_1 \\ u_2 \\ u_3 \\ u_4 \end{pmatrix} \tag{9}$$

So, the equation above is equivalent to the next form:

$$\dot{u} = Au \tag{10}$$

Where,

$$A = \begin{bmatrix} 0 & 0 & 1 & 0 \\ 0 & 0 & 0 & 1 \\ -\frac{K_{11}}{m} & -\frac{K_{12}}{m} & -\frac{C_{11}}{m} & -\frac{C_{12}}{m} \\ -\frac{K_{21}}{I_C} & -\frac{K_{22}}{I_C} & -\frac{C_{21}}{I_C} & -\frac{C_{22}}{I_C} \end{bmatrix} \tag{11}$$

This is the modal characteristic matrix of taper joint in the radial direction. Generally, the force between holder and spindle is the sum of elastic force and damping force, but elastic force is much larger than damping force [22]. In this way, joint modal characteristics equations are mainly determined by stiffness matrix. So, firstly, the joint can be considered approximately as an undamped system to obtain the elastic parameters. And then, the damping factors can be

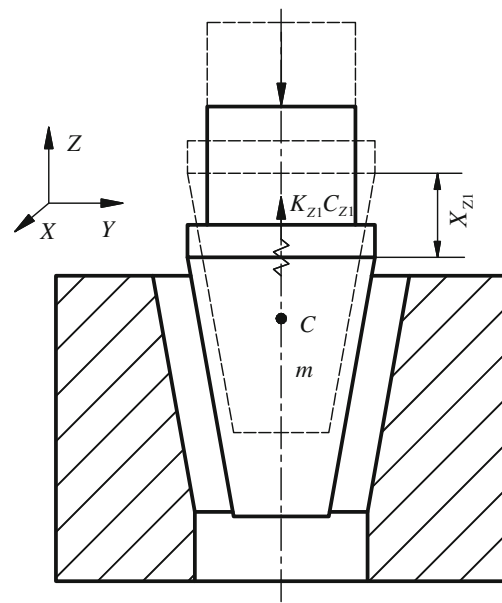


Fig. 5 Dynamic analysis in axial direction

calculated based on the natural frequencies and damping ratio by half-power method. The similar conclusion can be drawn in the Y section for the axisymmetric structure.

$$\begin{cases} \vec{K}_\theta = 4\pi^2 I_C \vec{f}_r \bullet \vec{f}_r \\ \vec{C}_\theta = 4\pi I_C \vec{f}_r \bullet \vec{\xi}_r \end{cases}$$

In axial direction, the joint is regarded as a single degree of freedom system shown in Fig. 5.

In this way, the dynamic equation in axial direction is given as following, where equivalent stiffness and damping is  $K_{Z1}$  and  $C_{Z1}$ :

$$m \ddot{X}_{Z1} + C_{Z1} \dot{X}_{Z1} + K_{Z1} X_{Z1} = 0 \tag{12}$$

Accordingly, the characteristic matrix is given as below.

$$A = \begin{bmatrix} 0 & 1 \\ -\frac{K_{Z1}}{m} & -\frac{C_{Z1}}{m} \end{bmatrix} \tag{13}$$

So, it is easy to get the stiffness and damping in axial direction.

$$K_{Z1} = m(2\pi f_n)^2 \tag{14}$$

$$C_{Z1} = 4\pi m f_n \xi \tag{15}$$

The dynamic characteristics with natural frequencies and damping ratios are obtained from FRF by impacting at the

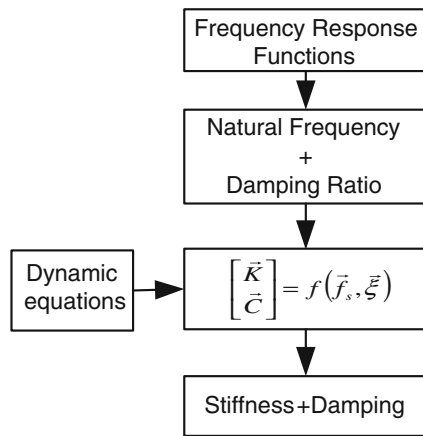


Fig. 6 Procedure of parameter identification

holder tip, and the joint parameters can be calculated from the above dynamic equations. Figure 6 shows the procedure of parameter identification.

First of all, the testing system measures the excitation and response at the same time to get the FRFs. Natural frequency and damping ratio are calculated from the FRFs by half-power point method. Moreover, combined with dynamic equations, the expressions between joint parameters and modal parameters are deduced. According to analysis above, it is available to calculate the unknown dynamic parameters of the joint if the FRFs can be obtain from experiment.

### 4 Experiment procedures

In order to obtain the parameters, the experiment platform for the spindle and holder is designed to meet the requirements of different pre-force and contact conditions, and the testing system of spindle–holder is shown in Fig. 7.

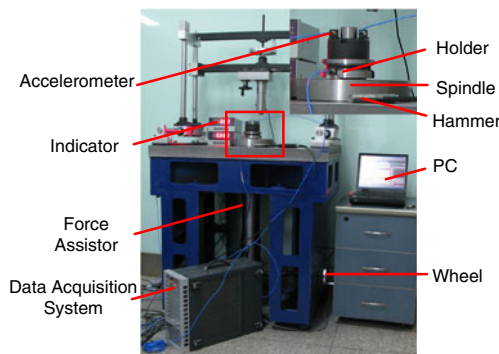


Fig. 7 Experiment setup

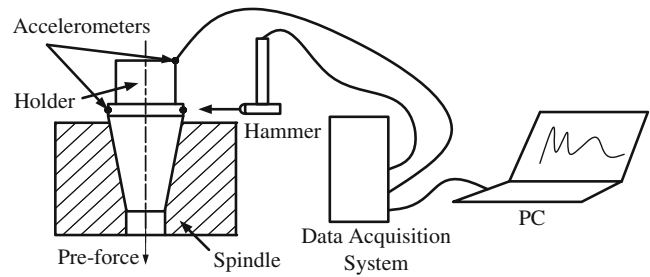


Fig. 8 Schematic of the testing system

This platform is designed for the analysis of spindle–holder system. Spindle and holder are both interchangeable parts to meet contact conditions of joint. And pre-force is generated by a wheel and transmitted to the end of holder by a stretchable universal joint, a turbine worm, and a screw. By this means, the platform generates pre-force from 0 to 40 kN easily, and the force is enough for the experiment. The schematic of the testing system is shown in Fig. 8.

Several accelerometers are installed on the end and the side of holder to measure the vibration signals. When hammer impacts on the holder, the translational and rotational movements are measured by the accelerometers because the end of holder express all the vibration modes including translation and rotation, where the rotation can be regarded as the product of the translation and the arm. Meanwhile, the data acquisition system (LMS test lab) collects the vibration signals of the hammer and accelerometers and transmits them to the PC. And it is necessary to set the pre-force at the end of the spindle through the wheel to ensure the stability. In this experiment, the pre-force varies from 0 to 25 kN, and the step is 1 kN. What is more, signals are averaged to identify FRFs to reduce random errors.

Theoretically, all points except for some static modal nodes are feasible to measure the response because those nodes vibrate in the same frequencies but different amplitudes.

The measure parameters are the most important prerequisites to obtain the real responses. In the study, the sample frequency is 20,480 Hz and the frequency resolution is 20 Hz. Ten impacts are averaged to reduce the random errors. The frequency spectrum generated by hammer requires even distribution to make sure that the power in all the frequency range is consistent. The hammer impacts on the holder in axial and radial independently. Especially, the hammer impacts the end face

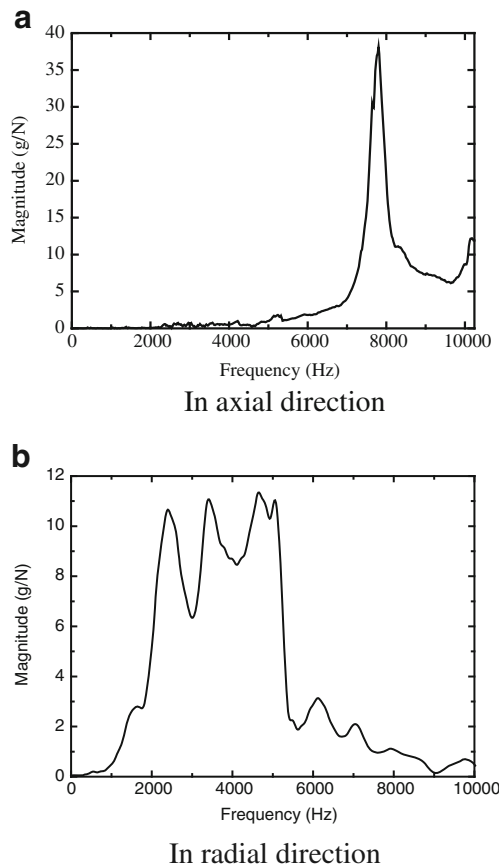


**Fig. 9** Frequency response function generated by hammer. **a** In axial direction. **b** In radial direction

of the holder in axial direction and the side face in radial direction. And the FRFs are shown in Fig. 9a, b, respectively, when the pre-force is 20 kN. From the FRFs, the natural frequency and damping are calculated by half-power method. The FRF in axial direction is early to identify the signal peak.

## 5 Experimental results

This section synthesizes the stiffness and damping with pre-force changing in axial and radial direction, respectively. All of the data are calculated from the experimental data to investigate the dynamic behaviors. It is found that the curves of FRF are similar in shape under the same condition except for the changing pre-force. And the peaks of FRF move to higher frequency as the pre-force increases. In this way,

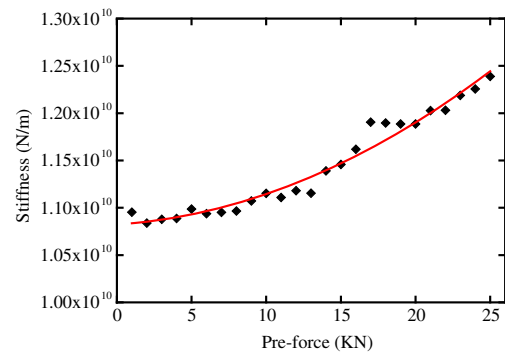


**Fig. 10** Axial stiffness with different pre-force

parameter data are collected and synthesized in the followings figures.

### 5.1 In axial direction

The stiffness of axial equivalent spring is varying from  $4.8 \times 10^9$  to  $5.0 \times 10^9$  N/m. The parameters of equivalent springs and damping with the changing pre-force are calculated and illustrated in Figs. 10 and 11.

It is illustrated that the stiffness increases together with the pre-force increasing. Furthermore, the change rate of stiffness  $dK/dF$  rises along with the pre-force increasing.

The damping ratios are calculated from the FRF by using the half-power method. By this means, the damping in axial direction varies from 1,000 N·s/m to 2,000 N·s/m. It is illustrated that the damping increases stably as the pre-force increases if it is less than

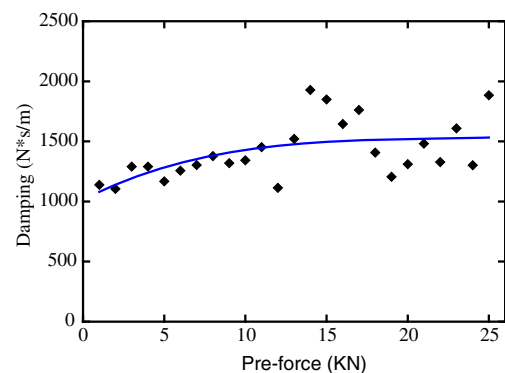


**Fig. 11** Axial damping with different pre-force

10 kN, but the damping is unstable when it is more than that.

### 5.2 In radial direction

Accordingly, the radial stiffness and damping are given in Figs. 12 and 13. The stiffness value in radial direction shows the same characteristics with that in axial direction, except that the rate of stiffness change  $dK/dF$  descends along with the pre-force increasing.

From the results, it is early to find that the pre-force influence the stiffness and damping to some extent. And the stiffness increases with the pre-force in both directions. Moreover, the damping increases in axial direction but decrease in radial direction. Specially, the variation law of the joint stiffness is called positive reinforce in this paper, which will influence the dynamic behavior in the machining process.

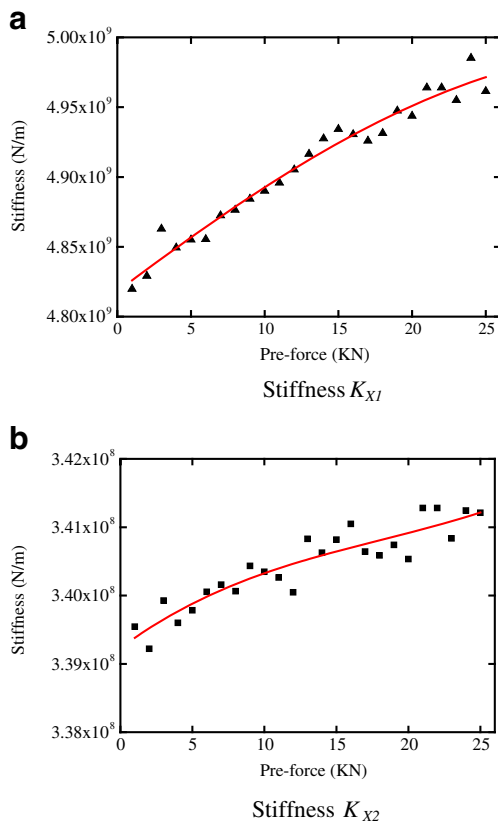


**Fig. 12** Radial stiffness with different pre-force. **a** Stiffness  $K_{X1}$ . **b** Stiffness  $K_{X2}$

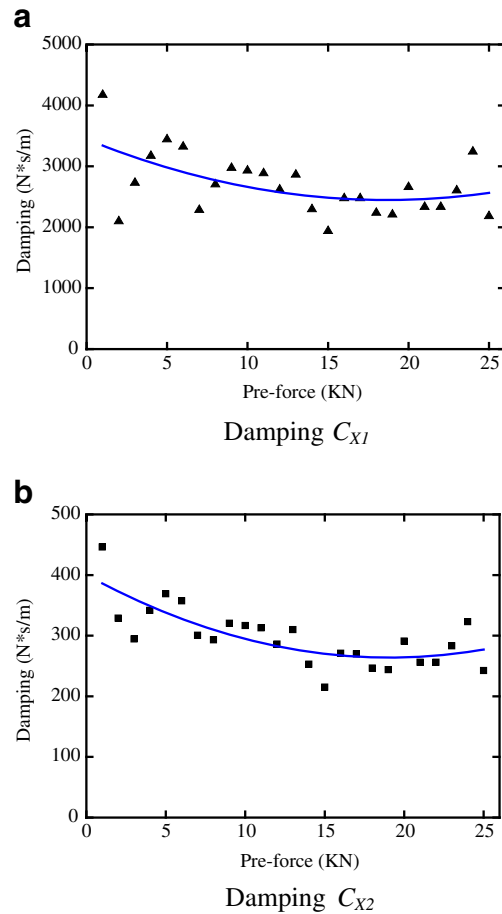


**Fig. 13** Radial damping with different pre-force **a** Damping  $C_{X1}$ . **b** Damping  $C_{X2}$

## 6 Discussions and validation

Based on the experiment results, this section discusses the change rule of stiffness in microstructure, and the simulation of the holder joint with the identified parameters for validation.

From the microscopic point, each joint can be regarded as rough surface with several peaks and hollows. When the normal force is applied on one part, the peaks and hollows contact with each other [23], which is shown in Fig. 14a. And it is assumed that the deformation of the structures themselves is smaller than the joint, so most of the deformation occurs in the joint. With the increase of normal force from  $F_1$  to  $F_2$ , the deformation of the top edge is  $\Delta X$ , shown in Fig. 14b. At the same time, the contact number increases accordingly, together with the increasing contact area. In this

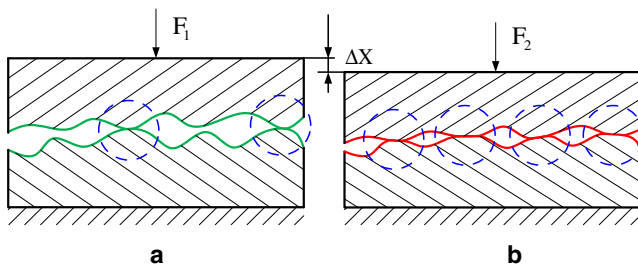


**Fig. 14** Microstructure explanation of stiffness characteristic

way, the small regions are reinforced to hinder the deformation.

So the conclusion is drawn that the contact stiffness rises more quickly because more contacts join in the interaction and larger area involves in the contact with the force increasing. Therefore, the change rate  $dK_n/dF$  increases as the increasing normal force. However, it is difficult to identify the variation of the damping because the stiffness effect covers the damping effect. To conclude, the damping is less important in the spindle–holder system, so the effect of the damping can be ignored in future analysis.

Similarly, the stiffness in the spindle holder system varies in the rule that the stiffness increases with the increasing external force. However, the holder can glide along the internal surface due to the 7/24 taper surface when impacted in the radial direction. Consequently, the stiffness increasing ratio reduces as a result of sliding.

In order to validate the accuracy of the joint parameters, FEM simulation is used to obtain the natural frequencies of spindle–holder system, and there are two models of joint parameters and bonded joint calculated respectively in this paper. The model of joint parameters is coupled with receptances, where the inner taper interface is connected with spring and damping elements, whose parameters are obtained from identification results. Figure 15a shows the way of model of joint parameters, where the pairs of spring

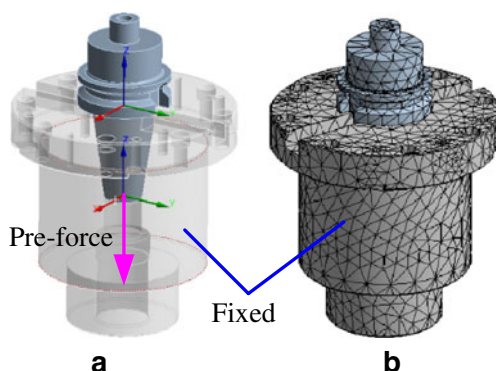


**Fig. 15** Model of spindle–holder system for simulation

and damping are located at the big and small end of the holder interface, and they are distributed equally on the interface according to the elements and nodes. However, the sum of the effect is as the same as that of located at the two ends. While, the joint in the model of the bonded joint connects the two parts tightly; consequently, the joint stiffness is equivalent to the stiffness of the material approximately. And this model is applied to verify the effectiveness of the joint parameters.

The FE model shown in Fig. 15b is calculated in ANSYS workbench for simulation, where the two different models are different from the joint setup and the fundamental model is the same for the comparison.

Furthermore, the two models keep the same boundary conditions and meshing. The cylindrical surface of the holder is fixed in order to keep the same conditions with those in the experiment. For the accuracy, the holder and the spindle is meshed with 3D 20-nodes-solid elements and shell elements. It is worth mentioning and investigating the natural frequency with the change pre-force because the frequency is the most important indicator for dynamic system.

In this way, the modal analysis is studied to obtain natural frequencies, where the joint parameters in simulation are based on the identification parameters from the experiment, and the joint in bonded is contact with each other closely just like one part without connections. The calculated results are shown in Fig. 16.

On one hand, it shows that the frequencies of simulation increase with the pre-force and the variation is consistent with the experiment, and the calculation errors are about 10 %. However, there is a difference between simulation and experiment because of the experimental error and assumptions. On the other hand, the bonded condition shows that the frequencies vary slightly with the pre-force increasing. Because the bonded joint makes the two parts contact closely together and the joint stiffness is close to that of the material. In

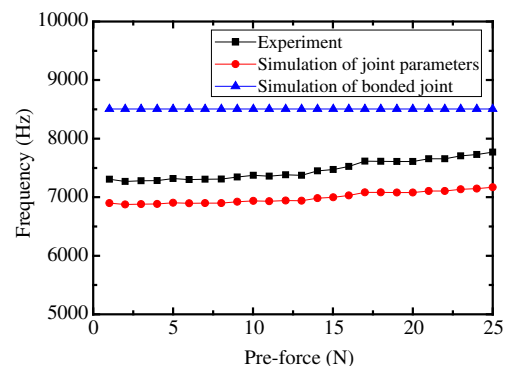


**Fig. 16** Frequencies validation of different conditions



this way, there will be more errors if joint parameters are ignored, but it is commonly used in some simulation software for its convenience. However, the frequencies with joint parameters are lower than those from the experiment. It is because of the assumption that the part is considered to be rigid body. The large stiffness of the parts themselves makes the small stiffness of the joint parameters values.

Even so, the precision of simulation is higher than bonded condition, furthermore, the pre-force is considered to improve the simulation. So, the joint parameters play an important role in improving the accuracy of the simulation.

## 7 Conclusions

This paper presents a new methodology to study the dynamic behaviors of the spindle–holder taper joint in dynamic modeling and parameters identification, where the pre-force at the end of holder is the main consideration. Firstly, a new dynamic model is proposed for the parameters identification of the spindle–holder taper joint, and the equivalent pairs of spring and damping are used to take the place of the original contact. Accordingly, the dynamic equations are given to describe the dynamic system. Secondly, this paper takes a BT 50 holder for example to carry out the experiment on the particular platform to identify parameters of stiffness and damping. Lastly, the rule of the dynamic stiffness with changing pre-load is discussed, and the positive reinforce effect suggests that the joint stiffness is increased along with the increasing normal force. Additionally, the precision of the joint parameters is confirmed in the way of FEM with obtained parameters.

The result shows that the joint parameters are applicable to simulate the dynamic behaviors of it before the real object is manufactured. For example, the harmonic response of the spindle system is calculated from the dynamic model with joint parameters to satisfy the stiffness requirement. In addition, we will pay more attention on how to use the parameters especially in simulation. More parameters related to more different spindle–holder system with different conditions are needed. Furthermore, all the parameters will be synthesized to find the mutual law for predicting behavior of a new holder. Above all, the parameters will be helpful for the designer to discover the advantages and the disadvantages before a real spindle is manufactured.

**Acknowledgments** This research is supported by the Key National Science and Technology Projects of China (grant no. 2012ZX04010-011).

## References

- Shamine DM, Shin YC (2000) Analysis of No. 50 taper joint stiffness under axial and radial loading. *J Manuf Process* 2(3):167–173
- Soliman E, Ismail F (1997) Chatter detection by monitoring spindle drive current. *Int J Adv Manuf Technol* 13(1):27–34
- Tamg YS, Hseih YW, Li TC (1996) Automatic selection of spindle speed for suppression of regenerative chatter in turning. *Int J Adv Manuf Technol* 11(1):12–17
- Bhuiyan SH, Choudhury IA, Yusoff N (2012) A new approach to investigate tool condition using dummy tool holder and sensor setup. *Int J Adv Manuf Technol* 61:465–479
- Seguy S, Insperger T, Arnaud L, Dessein G, Peigné G (2010) On the stability of high-speed milling with spindle speed variation. *Int J Adv Manuf Technol* 48:883–895
- Budak E, Ertürk A, Özgüven HN (2006) A modeling approach for analysis and improvement of spindle-holder-tool assembly dynamics. *Ann CIRP* 56(1):369–372
- Kim TR, Wu SM, Eman KF (1989) Identification of joint parameters for a taper joint. *J Eng Ind Trans* 111:282–287
- Rehom AG, Jiang J, Orban PE, Bordatchev E (2004) Modelling and experimental investigation of spindle and cutter dynamics for a high-precision machining center. *Int J Adv Manuf Technol* 11–12 (24):806–815
- Agapiou JS (2005) A methodology to measure joint stiffness parameters for toolholder–spindle interfaces. *J Manuf Syst* 24:13–20
- Ahmadi K, Ahmadian H (2007) Modelling machine tool dynamics using a distributed parameter tool–holder joint interface. *Int J Mach Tool Manuf* 47:1916–1928
- Ahmadian H, Nourmohammadi M (2010) Tool point dynamics prediction by a three-component model utilizing distributed joint interfaces. *Int J Mach Tool Manuf* 50:998–1005
- Forestier F, Gagnol V, Ray P, Paris H (2012) Model-based cutting prediction for a self-vibratory drilling head–spindle system. *Int J Mach Tool Manuf* 52:59–68
- Schmitz T, Donaldson R (2000) Predicting high-speed machining dynamics by substructure analysis. *Ann CIRP* 49 (1):303–308
- Altintas Y, Cao Y (2005) Virtual design and optimization of machine tool spindles. *CIRP Ann* 54:379–382
- Burns TJ, Schmitz TL (2005) A study of linear joint and tool models in spindle-holder-tool receptance coupling. *ASME 2005 International Design Engineering Technical Conferences and Computers and Information in Engineering Conference (IDETC/CIE2005)* 6:947–954
- Ertürk A, Özgüven HN, Budak E (2006) Analytical modeling of spindle–tool dynamics on machine tools using Timoshenko beam model and receptance coupling for the prediction of tool point FRF. *Int J Mach Tool Manuf* 46:1901–1912
- Ertürk A, Budak E, Özgüven HN (2007) Selection of design and operational parameters in spindle–holder–tool assemblies for maximum chatter stability by using a new analytical model. *Int J Mach Tool Manuf* 47:1401–1409
- Özsahin O, Ertürk A, Özgüven HN, Budak E (2009) A closed-form approach for identification of dynamical contact parameters in spindle–holder–tool assemblies. *Int J Mach Tool Manuf* 49:25–35
- Namazia M, Altintas Y, Abe T, Rajapakse N (2007) Modeling and identification of tool holder–spindle interface dynamics. *Int J Mach Tool Manuf* 47:1333–1341
- Agapiou J, Rivin E, Xie C (1995) Toolholder/spindle interfaces for CNC machine tools. *Ann CIRP* 4(1):383–387
- Greenwood JA, Williamson JBP (1966) Contact of nominally flat surfaces. *Proc R Soc Lond* 295:300–317
- Vu-Quoc L, Zhang X (1999) An elastoplastic contact force–displacement model in the normal direction: displacement–driven version. *Proc R Soc Lond* 455:4013–4044
- Cao T, Sutherland JW, Zheng Y (1996) An experimental investigation into the effect of joint conditions on structural damping with application to machine tools. *Proc of 2nd SM Wu Symposium on Manufacturing Science* 2:122–127